Polymer 51 (2010) 2069–2076

Contents lists available at ScienceDirect

Polymer

journal homepage: www.elsevier.com/locate/polymer

Evolution of interphase in styrene-butadiene block copolymers as revealed by ^{1}H solid-state NMR: Effect of temperature and molecular architecture

Weigui Fu [a], Run Jiang [a], Tiehong Chen [b], Hai Lin [b], Pingchuan Sun [b,*], Baohui Li [a,*], Qinghua Jin [a], Datong Ding [a]

[a] College of Physics, Nankai University, Tianjin, 300071, China
[b] Key Laboratory of Functional Polymer Materials, Ministry of Education, Institute of Polymer Chemistry and College of Chemistry, Nankai University, Tianjin, 300071, China

ARTICLE INFO

Article history:
Received 1 October 2009
Received in revised form
25 January 2010
Accepted 1 March 2010
Available online 9 March 2010

Keywords:
Block copolymer
Interphase
Solid-state NMR

ABSTRACT

^{1}H spin-diffusion solid-state NMR, in combination with other techniques, was utilized to investigate the effect of molecular architecture and temperature on the interphase thickness and domain size in poly (styrene)-*block*-poly(butadiene) and poly(styrene)-*block*-poly(butadiene)-*block*-poly(styrene) copolymers (SB and SBS) over the temperature range from 25 to 80 °C. These two block copolymers contain equal PS weight fraction of 32 wt%, and especially, polystyrene (PS) and polybutadiene (PB) blocks are in glass and melt state, respectively, within the experimental temperature range. It was found that the domain sizes of the dispersed phase and interphase thicknesses in these two block copolymers increased with increasing temperature. Surprisingly we found that the interphase thicknesses in these two block copolymers were obviously different, which was inconsistent with the theoretical predictions about the evolution of interphase in block copolymer melts by self-consistent mean-field theory (SCFT). This implies that the interphase thickness not only depends strongly on the binary thermodynamic interaction (χ) between the PS and PB blocks, but also is influenced by their molecular architectures in the experimental temperature range.

1. Introduction

In heterogeneous polymer systems, such as multicomponent and multiphase polymers, the interphase between adjacent phases is an important factor in determining many physical properties in such materials [1]. The interphases are not only highly dependent on the compatibility of the components, but also influenced by heat treatment, aging and molecular architectures. Characterizing the temperature dependence of nanoscale interphase is very important for understanding the relationship between microscopic structure and macroscopic behavior, which will help polymers blend effectively integrated into modern technologies.

Various theories concerning the quantitative relationship between the interphase thickness d_{itp} and the thermodynamic interaction parameter χ for immiscible polymer pairs have been proposed in the past decades. In the early 1970s, Helfand et al. [2,3] first constructed a self-consistent mean-field theory (SCFT) of polymer–polymer interphase. The finite molecular weight effect of the components was further considered theoretically by Broseta et al. [4]

$$d_{itp} = \frac{2b}{(6\chi)^{1/2}}\left[1+\frac{\ln 2}{\chi}\left(\frac{1}{N_A}+\frac{1}{N_B}\right)\right] \quad (1)$$

where b is the Kuhn segment length (effective length of per monomer unit, 0.8 nm) [3,4], N_i (i = A, B) is the number of segments of each block and the Flory–Huggins interaction parameter, χ, usually depends on temperature, blend composition and component molecular weights [5]. The interphase in block copolymers comprised of incompatible blocks has been attracted significant attention in the past decades [6,7], since such materials are increasingly being used as compatibilizers, surfactants, and adhesives in polymer industry. A more general theoretical work by SCFT method for block copolymer melts were reported by Matsen et al. [8], and such calculations indicated the similar interphase thickness for the AB and ABA copolymers in lamellar phase. On the basis of this theoretical work, the evolution of the interphase under different χ in heterogeneous polymer melts can be well understood.

Due to the extremely small volume fraction of the interphase in a typical polymer blend, experimental determination of interphase thickness is still a challenge. A variety of experimental techniques including small-angle X-ray scattering (SAXS) [9], dynamic mechanical measurements [10], transmission electron microscopy

* Corresponding author. Tel.: +86 22 23508171; fax: +86 22 23494422. ;
E-mail addresses: spclbh@nankai.edu.cn (P. Sun), baohui@nankai.edu.cn (B. Li).

0032-3861/$ – see front matter © 2010 Elsevier Ltd. All rights reserved.
doi:10.1016/j.polymer.2010.03.009

(TEM) [11], fluorescence spectroscopy [12], thermal methods [13], small-angle neutron reflectivity (SANS) [14], oxygen permeability [15], ellipsometry [16] and nuclear magnetic resonance(NMR) [17,18] were utilized to investigate the thickness and composition of interphase. Most of the existing theoretical and experimental results agreed that the interphase thickness of immiscible polymers could range from a few to tens of nanometers [7,19]. Solid-state NMR (SSNMR) spectroscopy has been proved to be a non-destructive and powerful technique to study the structure and dynamics of polymers [20,21]. The work of Zumbulyadis [1] group has determined the interphase mixing in symmetric diblock copolymers based on the $^{1}H-^{2}H$ cross-polarization and magic angle spinning (CP-MAS) NMR approach. Based on the differences in molecular mobility in different phases, proton spin-diffusion NMR experiments have been extensively applied to investigate the microphase structure in multiphase solid polymers, such as polymer blends [22,23], block copolymers [24,25], core-shell polymers [26] and so on. Models that capture the essence of the spin-diffusion process have been proposed [27,28]. Very recently, a novel NMR method using high-resolution MAS and double-quantum filtered ^{1}H spin-diffusion was used to study the component profile in the interfacial region in block copolymers [29]. In spite of these previous studies, little experimental work was reported to investigate the evolution of interphase in block copolymer with different molecular architectures where the two blocks were in the state of glass and melt, respectively, at a special temperature range. This temperature range is very important for practical applications of the block copolymer in industrial field. The combination of glass and melt state enable us to prepare tough material, which is widely used in our everyday life (e.g. High Impact Polystyrene, HIPS). The nanoscale interphase properties for block copolymers in such temperature range are still far from being well understood, therefore, detailed information about these issues needs to be further elucidated.

In traditional NMR works, interphase thickness can be determined by computer simulation of the measured spin-diffusion data [30], however, this method needed a specific diffusion model and was not suitable to small interphase (e.g. <1 nm). Recently, we have developed a new method to determine interphase thickness by using dipolar filtered and spin-diffusion ^{1}H SSNMR [22]. The key point is that the immobilized component in interfacial region can be determined by varying dipolar filter strength in spin-diffusion experiment, and the interphase thickness can then be directly calculated from a strict mathematic relationship between interphase and domain size. The above method has been successfully used to characterize the influence of binary polymer–polymer interaction on the phase behavior, domain size and especially the interphase

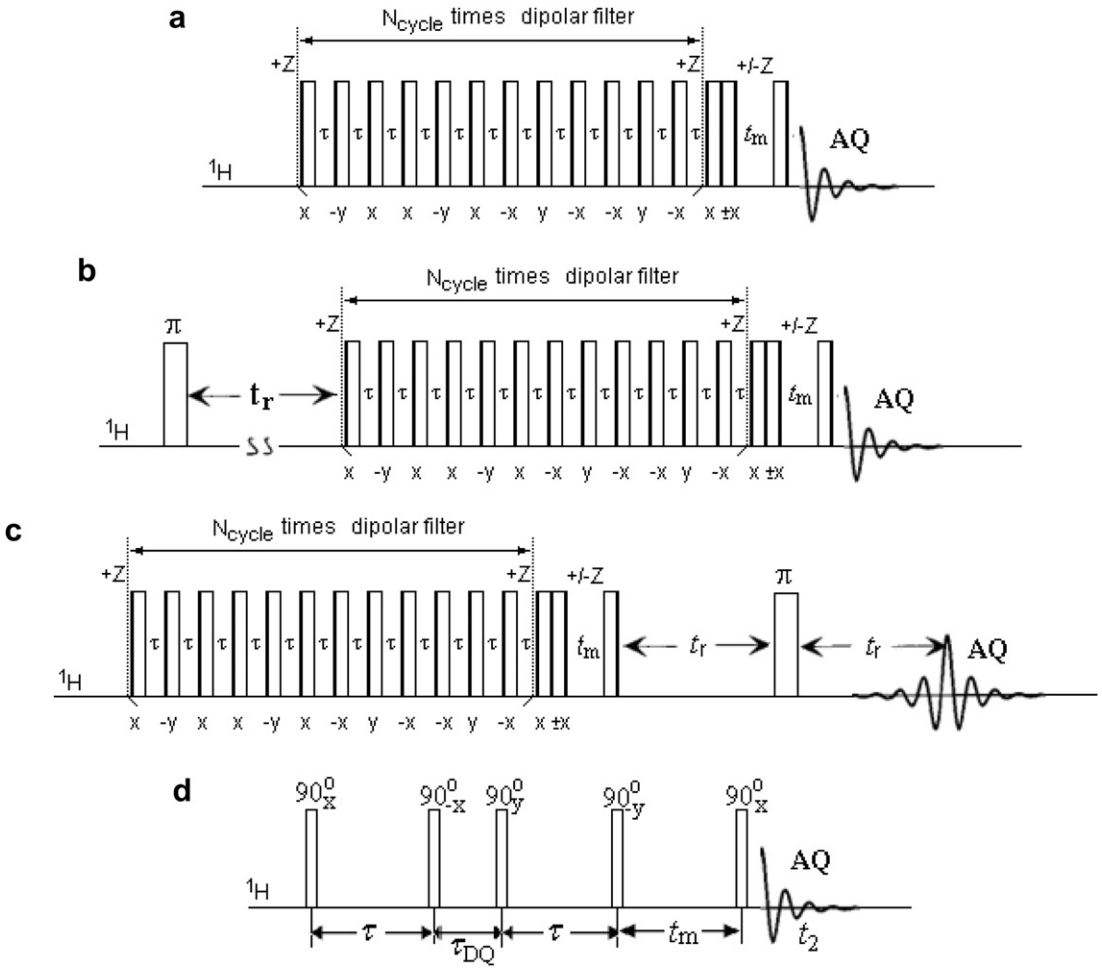

Fig. 1. (a) Pulse sequence with a 12-pulse dipolar filter for ^{1}H dipolar filter and spin-diffusion experiment, (b) pulse sequence to measure T_1 of the mobile phase (t_r was varied), (c) dipolar filtered Hahn spin echo pulse sequence to measure T_2 of the mobile phase and (d) pulse sequence to measure the line width of the ^{1}H spectrum with a five-pulse double-quantum (DQ) filter.

thickness in thermoset blends ER/PE-PPO-PEO and UPR/PEO-PPO-PEO with weak and strong microphase separation, respectively [22]. In this work, we aim to use the above NMR method to further elucidate the influence of temperature and molecular architecture on the interphase thickness in diblock and triblock copolymers of styrene and butadiene (SB and SBS). These two block copolymers contain equal PS weight fraction (32 wt%), which forms a microphase structure of the rigid PS domain dispersed in the mobile PB matrix. The selected experimental temperature range in this work is choose from 25 to 80 °C, *where PS and PB blocks are in glass and melt state*, *respectively*. The NMR results were then compared with previous theoretical results for the immisible block copolymer melts studied by SCFT, which may provide new insight into the interphase behavior for block copolymers with glass and melt blocks, respectively.

2. Experimental

2.1. Materials and preparation of samples

Poly(styrene-b-butadiene) (SB) diblock (Molecular weight, $M_w = 73{,}930$ g/mol; Polydipersity index, PI = 1.1) and the matching (styrene-b-butadiene-b-styrene) (SBS) triblock ($M_w = 140{,}000$ g/mol, PI = 1.2) copolymers having equal polystyrene (PS) weight fraction [31,32] were purchased from Aldrich Chemical Co. The calibrated weight fraction of styrene in SB and SBS by ^{1}H liquid-state NMR in $CDCl_3$ was 32 wt% as shown in Figure S1 in Supplementary material. The samples were annealed under vacuum at 120 °C for 10 h and gradually cooled to room temperature for NMR experiments. The glass transition temperatures of the samples were measured by differential scanning calorimetry (DSC, NETZSCH DSC 204) as shown in Figure S2 in Supplementary material.

2.2. Small-angle X-ray scattering (SAXS) experiment

All SAXS experiments were performed on a Bruker Nanostar small-angle X-ray scattering system consisting of Siemens X-ray (40 kV and 35 mA), operating at a 0.154 nm wavelength (λ) for Cu K_α radiation. The sample-to-detector distance is 106.35 cm. The plot of SAXS intensity was presented as a function of the scattering wave vector, q ($=4\pi \sin\theta/\lambda$, where 2θ is the scattering angle). The long period, d_L, is inversely related to q, $d_L = 2\pi/q$. The domain size of the dispersed phase, d_{dis}, can be calculated from the relationship $d_L = 1.0\phi_S^{-1}d_{dis}$ (lamella) and $d_L = 0.95\phi_S^{-1/2}d_{dis}$(cylinder), respectively, where φ_S is the volume fraction. An alternative method to calculate d_L and d_{dis} using the correlation function obtained from SAXS profile is also given in Supplementary material as shown in Figure S3. The temperatures were set at ranging from 25 to 80 °C, a temperature equilibration period of 2 h was used before SAXS data were acquired at each measurement temperature.

2.3. Transmission electron microscopy (TEM) experiment

All TEM experiments were performed on a H-800 transmission electron microscope, operating at acceleration voltage of 200 kV. Sections 70–100 nm thick were obtained by slicing the sample with a diamond knife at −110 °C. To enhance the contrast of the images, the samples were stained for 40 mins in an OsO_4 solution, which selectively reacts with the double bond of PB and stays with it. The dark regions of the brightfield TEM images are identifiable with the polybutadiene (PB) domains whereas the bright regions are PS.

2.4. NMR experiments

Liquid-state NMR experiments were carried out on a UNITYplus-400 narrow-bore (54 mm) NMR spectrometer operating at a proton frequency of 400.1 MHz, all samples were dissolved in $CDCl_3$. Solid-state NMR experiments were performed on a Varian Infinityplus-400 wide-bore (89 mm) NMR spectrometer operating at a proton frequency of 399.7 MHz. A conventional 4 mm double-resonance CP/MAS T3 NMR probe was used for all experiments, and samples were placed in a 4 mm zirconia PENCIL rotor with 52 μl sample volume. Variable-temperature ^{1}H SSNMR experiments were carried out in the temperature range of 25–80 °C with a Varian Model-L950 temperature controller, a temperature equilibration period of 10 min was used before NMR spectra were acquired at each measurement temperature. Furthermore, we find that a longer equilibration period of 2 h does not change the result. All the NMR data were processed with Varian Spinsight software. The ^{1}H chemical shifts were referenced to external TMS. The pulse sequences for solid-state NMR experiments shown in Fig. 1 are the same as used in our previous work [22] and Ref. [23], and briefly described below.

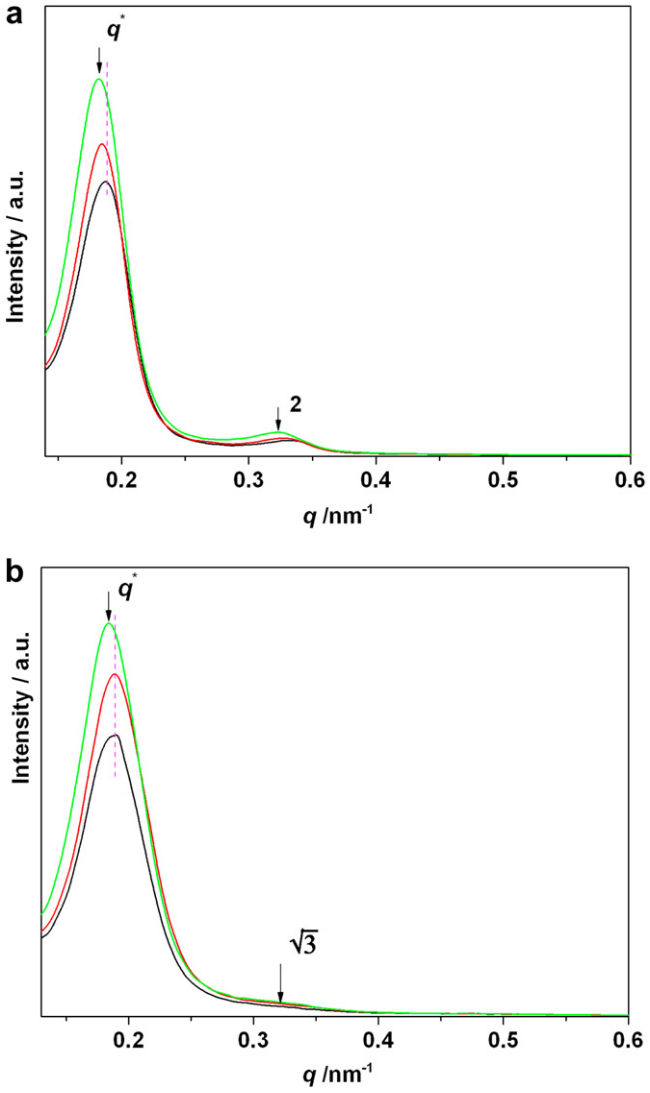

Fig. 2. Temperature dependence of SAXS profiles for (a) SB and (b) SBS block copolymers. Temperatures from top to bottom are 80, 50 and 25 °C, respectively. The peak ratios (relative to the first peak position marked as q^*) for the corresponding ordered structures are indicated by arrows.

Proton spin-diffusion experiments [27,34,35] with a 12-pulse dipolar filter [35] were used to achieve a magnetization modulation across a dynamically heterogeneous sample (Fig. 1a). The dipolar filter with several cycles selects the ^{1}H magnetization from the mobile phase with low glass transition temperature (T_g), which has longer transverse relaxation times than those of rigid phase with a higher T_g. After application of the 12-pulses dipolar filter, a pair of 90° pulses was then placed immediately with 0° and 180° phase-cycled in order to eliminate the effect of T_1 relaxation during the mixing period. The following step is a "mixing" period (t_m), in which the remaining proton magnetization stored on the $\pm Z$ axis diffuses to neighboring spins and eventually reach an equilibration of the inhomogeneous magnetization distribution. The final step is the direct ^{1}H detection. The domain sizes can be determined using proton spin-diffusion when the polarization gradient is relaxed. The effects of T_1 relaxation were removed from the spin-diffusion decay curve by making use of T_1 values, which were independently measured using a inversion-recovery sequence before the dipolar filter (Fig. 1b) with a recycle delay of 3–5T_1. The 90° pulse length in dipolar filter is 2.5 μs and the inter-pulse spacing of τ is typically 15 μs. All spin-diffusion experiments in this work were performed under static conditions to avoid being influenced by MAS [20,30,36]. The spin-diffusion coefficients of the mobile PB phase were determined by the transverse relaxation time (T_2), which were measured by ^{1}H dipolar filtered Hahn-echo NMR experiments [33] (Fig. 1c). For the minor rigid component, PS, its spin-diffusion coefficients were obtained by measuring the line widths of proton NMR signals with double-quantum (DQ) filter pulse sequence (Fig. 1d) [37], where τ is the excitation and reconversion time, and t_{DQ} is the evolution time (3 μs). The determination of the interphase thickness in multiphase polymers by ^{1}H spin-diffusion SSNMR was performed by using our previous method [22].

3. Results and discussion

3.1. Phase behavior, morphology and microdomain structure characterized by SAXS and TEM experiments

SAXS and TEM are traditional and convenient methods to determine the phase behavior, morphology and microdomain structure of multiphase polymers. SAXS experiments were first used to identify the ordered microstructure of SB and SBS. Fig. 2 shows the typical scattered intensity $I(q)$ profiles against wave vector (q) for the two block copolymers measured at temperatures ranging from 25 to 80 °C. With increasing temperature, the primary peak intensity increases, and higher order reflections develop. Furthermore, all peak positions shift to the left (lower q value) for both SB and SBS, indicating an increase in domain spacing d_L ($=2\pi/q$). The peak ratio (relative to the first peak position marked as q^*) in Fig. 2a is 1:2, indicating an ordered lamellar structure in SB. The calculated d_L and domain size of the dispersed phase (d_{dis}) are 33–35 nm and 9–11 nm at temperatures ranging from 25 to 80 °C, respectively. For SBS triblock copolymer, the peak ratio as show in Fig. 2b is $1:\sqrt{3}$, indicating a hexagonally packed cylindrical morphology. The calculated d_L and d_{dis} are 33–34 nm and 19–20 nm at temperatures ranging from 25 to 80 °C, respectively.

The morphology of the studied samples can be observed directly by TEM. Fig. 3 displays the TEM images obtained for the SB and SBS, respectively, which evidently reveal that there are ordered phase separation structures in these two samples. The dark areas are the PB microphases which can be preferentially stained with OsO_4 compared to the rigid PS phases. On the basis of Fig. 3, one may thus conclude that the microstructures for SB and SBS are lamellar and cylinders-like structures, respectively. The long period, d_L, of the lamella or cylinder in these two samples is about 30–35 nm. The TEM experimental results are in good agreement with that obtained from the above SAXS experiments. Although TEM experiments provide direct information about the morphology, it is difficult to determine the interphase thickness and monitor its temperature dependence. In the following section, the ^{1}H spin-diffusion experiments enable us to quantitatively determine the interphase thickness and its temperature dependence.

3.2. Solid-state NMR study of domain size and interphase thickness

In our previous work on thermoset blends containing triblock copolymers (ER/PEO-PPO-PEO and UPR/PEO-PPO-PEO) [22], we developed a new method based on ^{1}H spin-diffusion experiments to quantitatively determine the interphase thickness in multiphase polymers containing rigid and mobile components. For SB and SBS

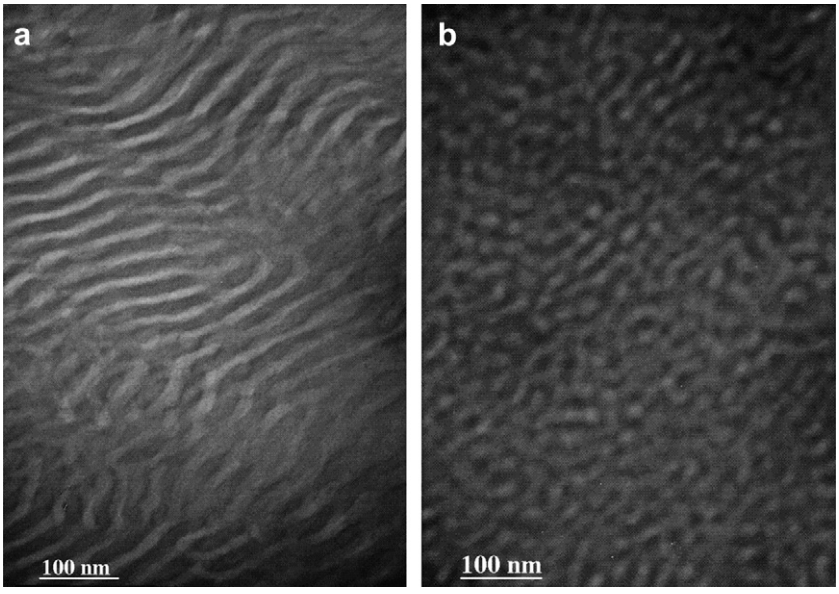

Fig. 3. TEM micrograph of (a) SB and (b) SBS. The specimen for TEM observation was stained with OsO_4 and the scale bar is 100 nm.

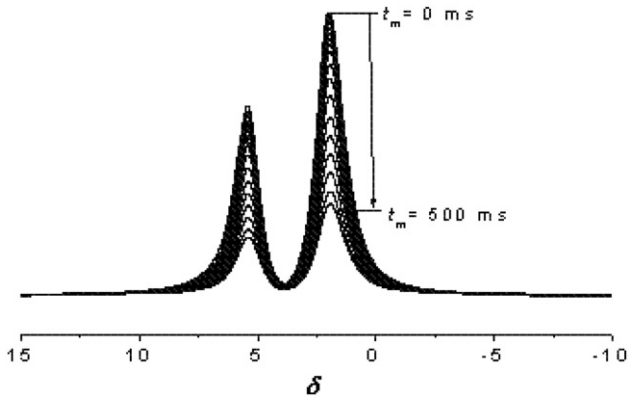

Fig. 4. 400 MHz solid-state ^{1}H spin-diffusion NMR spectra of PS–PB with increasing mixing time t_{mix} from 1 to 500 ms under $N_{cycle} = 10$.

block copolymers, the rigid PS phase is expected to disperse in mobile PB matrix as indicated by TEM results.

Before carrying out the spin-diffusion experiments, the stoichiometric proton ratio (75.0%) of the mobile PB in the SB and SBS block copolymers was determined by ^{1}H liquid-state NMR. Fig. 4 presents the typical static spin-diffusion spectra at mixing time t_m from 1 to 500 ms for SB with $N_{cycle} = 10$ and $\tau = 15$ μs. The spin-diffusion cures for SB and SBS at different filter strengths are shown in Figure S4 in Supplementary material.

Fig. 5 shows the selected fraction in spin-diffusion experiments for the samples with different filter strength (N_{cycle}) (the ^{1}H spin-diffusion curves with increasing dipolar filter strength (N_{cycle}) are shown in Figure S4 in Supplementary material). The final value (69.0% at $N_{cycle} > 10$) is slightly lower than that expected from the stoichiometric proton ratio (75.0%), indicating the strong phase separation and the existence of a small interphase region in the block copolymers, this behavior is similar with that of UPR/PEO-PPO-PEO blend in our previous studies [22].

In our previous work, a strict mathematical relationship between interphase thickness, d_{itp}, and the domain size of dispersed phase, d_{dis}, was established as

$$d_{itp} = \left(\sqrt[p]{2-\lambda_{DFS}} - \sqrt[p]{\lambda_{DFS}}\right) d_{dis}/2 \quad (2)$$

where the parameter λ_{DFS} represents the residual proton fraction of mobile phase in stoichiometric mobile phase, which can be directly measured by ^{1}H NMR experiments as shown in Fig. 5, p represents the dimensions (1, 2, 3). For dispersed rigid phase (d_{dis}), such as the case in SB and SBS used in this work, λ_{DFS} is simply changed to $(f_{sr} - f_i)/f_{sr} = 1 - f_i/f_{sr}$. Where f_{sr} is the stoichiometric proton fraction of dispersed rigid phase as shown in Fig. 5.

Traditional NMR strategy can be used to determine d_{dis} if SAXS and TEM cannot provide quantitative structural information due to either lower electron density contrast or low stain contrast between different phases, such as the case for ER/EO80 in our previous work [22]. The domain size of the discrete phase B in the two-phase A/B mixture, d_{dis}, can be determined by the following equation

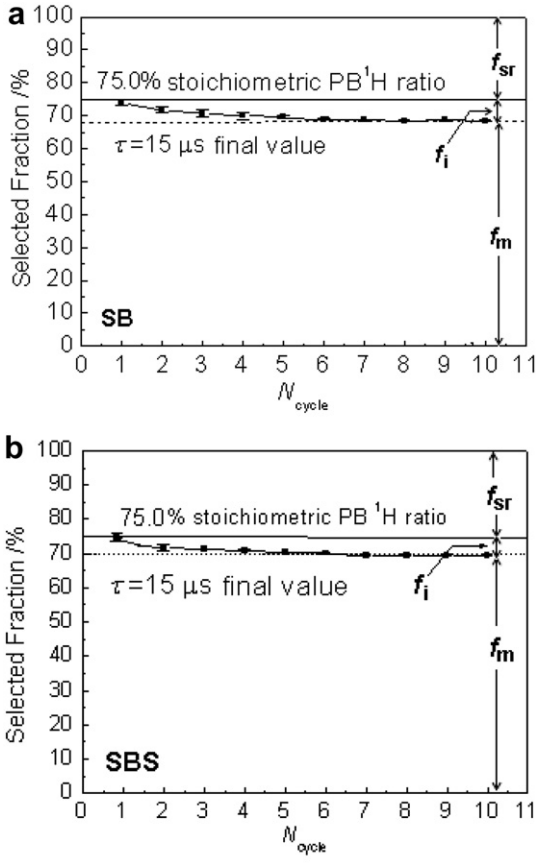

Fig. 5. Selected fraction as the function of filter strength (N_{cycle}) for (a) SB and (b) SBS at room temperature.

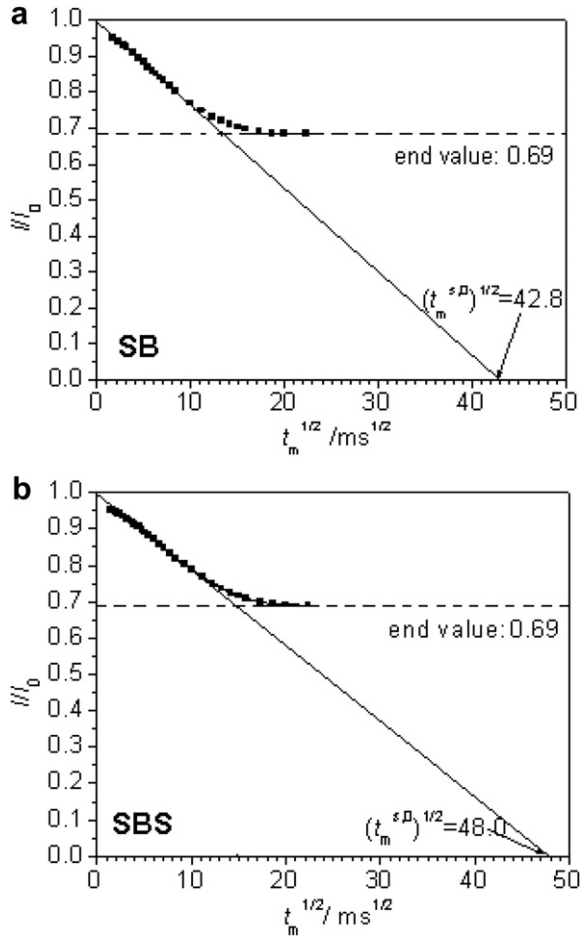

Fig. 6. Spin-diffusion curves, plotted as the normalized intensity I/I_0 against the square root of the mixing time t_m for (a) SB and (b) SBS with $N_{cycle} = 10$ at room temperature.

Table 1
Volume fraction, and proton density used to calculate the domain size.

Parameters[a]	ϕ_{PS}	ρ^{H}_{PS} (g/cm^3)	ρ^{H}_{PB} (g/cm^3)
PS–PB PS–PB–PS	0.318	0.081	0.112

[a] (a) ϕ_{PS} is the volume fraction of the rigid phase PS, which can be calculated from the 32.5% weight ratio of PS, as well as the density for PS and PB of 1.05, 1.01 g/cm^3, respectively. (b) ρ^{H}_{PS} and ρ^{H}_{PB} are the proton density for the PS and PB, respectively.

$$d_{dis} = \phi_B/\phi_A \times \varepsilon \times \sqrt{4D_{eff}t_m^{s,0}/\pi} \quad (3)$$

where ϕ_m ($m = A, B$) is the volume fraction of the mobile phase A or rigid phase B. The ε represents the dimensionality, and its value depends on the morphology and is 1 for lamellar, 2 for cylindrical, and 3 for spheres (or cubes) in a matrix. $t_m^{s,0}$ is the characteristic mixing time of spin-diffusion introduced by Mellinger et al. [34], and it can be determined by the intercept of the extrapolated linear initial decay with the *X*-axis in the spin-diffusion curves, as shown in Fig. 6. Fig. 6 presents the spin-diffusion plots for the SB and the SBS, respectively. The initial linear portion of the curve is extrapolated to give a $(t_m^{s,0})^{1/2}$ value of 42.8 ms$^{1/2}$ for SB, and 48.0 ms$^{1/2}$ for SBS at room temperature. The effective spin-diffusion coefficient D_{eff} is defined according to the following equation

$$\sqrt{D_{eff}} = \frac{2\sqrt{D_A D_B}}{(\rho_A^H/\rho_B^H)\sqrt{D_A} + \sqrt{D_B}} \quad (4)$$

where, ρ_A^H and ρ_B^H are proton densities. The spin-diffusion coefficient of the mobile and rigid phase, denoted as D_A and D_B here, respectively. Table 1 lists some of the parameters used in the spin-diffusion calculations.

3.2.1. Temperature effect on the ^{1}H spin-diffusivity

In order to calibrate spin-diffusion data by T_1 as shown in Fig. 6, we further measured the ^{1}H relaxation times of PB as well as the ^{1}H line width of the rigid PS in all samples at the temperature range from 25 to 80 °C. The resulting of T_1 for SB (black line) and SBS (red line) are plotted against the temperature in Fig. 7a. Since spin-diffusion coefficients will change with increasing temperature, therefore, the spin-diffusion coefficients should be determined at different temperatures for accurate analysis of domain size and interphase thickness in the block copolymers as a function of temperature. For the mobile fractions of SB, the spin-diffusion coefficients of D_A can be calculated from the following equations proposed by Mellinger et al. [34] through transverse relaxation time (T_2) measurements:

$$D_A\left(T_2^{-1}\right) = \left(8.2{*}10^{-6}T_2^{-1.5} + 0.007\right)\ \mathrm{nm^2/ms}, \quad 0 < T_2^{-1} < 1000\ \mathrm{Hz} \quad (5)$$

$$D_A\left(T_2^{-1}\right) = \left(4.4{*}10^{-5}T_2^{-1} + 0.26\right)\mathrm{nm^2/ms}, \quad 1000 < T_2^{-1} < 3500\ \mathrm{Hz} \quad (6)$$

Fig. 7b, c shows the temperature dependence of the T_2 relaxation time and the spin-diffusion coefficient in the range of 25–80 °C, respectively. Upon increasing temperature, the T_2

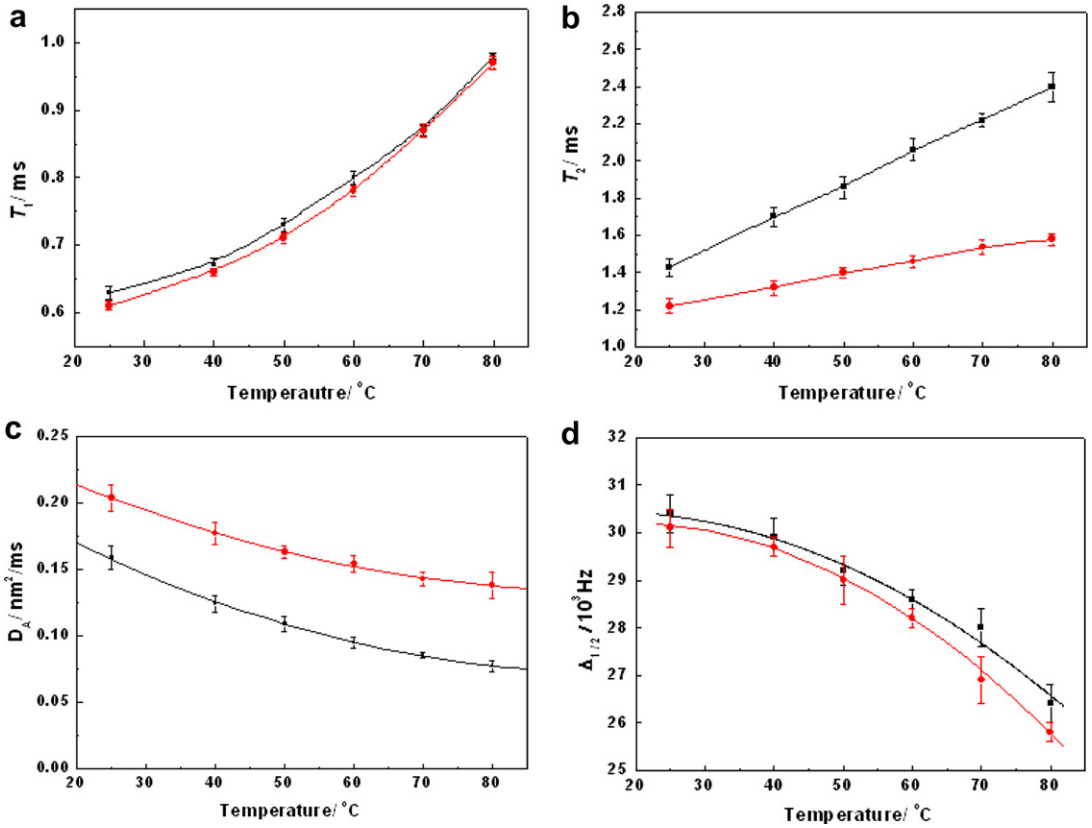

Fig. 7. Temperature dependence of the ^{1}H relaxation time T_1 (a), T_2 (b) and the ^{1}H spin-diffusion coefficient of the soft fraction (c), and the ^{1}H line width of the rigid phase (d) for the SB (■) and SBS (●).

relaxation time increases, and the calculated spin-diffusion coefficient decreases due to an increase in the molecular mobility. It implies that the PB block in SB is more mobile, for the T_2 relaxation time of the PB in SB is longer than that of the SBS. That agrees with the comparing results of T_1 for SB and SBS.

The diffusion coefficient of the rigid phase (D_B) can be calculated from the following equation that is valid for the Gaussian line shape [37]

$$D_B = k < r^2 > \Delta\nu_{1/2}^B \quad (7)$$

where k is a numerical factor. This relation is valid only for a Gaussian NMR absorption spectrum. $<r^2>$ is the mean-square distance between the nearest spins (typically be of the order of 0.04–0.06 nm^2 in polymer), $\Delta\nu_{1/2}^B$ is the full width at half height of proton signals obtained by solid-state ^{1}H NMR experiment with double-quantum (DQ) filter [38]. The diffusivity can be readjusted for the rigid phase using the scaling relation Eq. (8).

$$D_B = D_{ref} \times \frac{< r^2 >_B}{< r^2 >_{ref}} \times \frac{\Delta\nu_{1/2}^B}{\Delta\nu_{1/2}^{ref}} \quad (8)$$

The reference material used here is a PMMA-PS diblock copolymer[24] with $D_{ref} = 0.8 \pm 0.2$ nm^2/ms, $\Delta\nu_{1/2}^{ref} = 38$ kHz, and $<r^2>_{ref} = 0.0625$ nm^2. Fig. 7d shows the decrease of $\Delta\nu_{1/2}^B$ for the PS block with increasing temperature, which indicates that D_B is influenced by temperature (not shown here).

3.2.2. Temperature dependence of the domain size and the interphase thickness

In order to investigate the temperature effect on the domain size and interphase thickness, ^{1}H spin-diffusion experiment was performed for SB and SBS at temperatures ranging from 25 to 80 °C. Fig. 8a shows the temperature dependence of the domain size of dispersed phase, d_{dis}. The d_{dis} increases with increasing temperature for both SB and SBS, which is consistent with that of the SAXS results. Furthermore, the d_{dis} values for the triblock copolymer are larger than that of the diblock copolymer.

Fig. 8b indicates that the interphase thicknesses (d_{itp}) increase with increasing temperature in SB diblock copolymer and its SBS triblock counterpart. It is well known that the binaural component interaction (χ) is the key factor controlling the final microstructure and morphologies of the phase separation [39]. The χ parameter is usually a function of temperature, T(K), which can be written (empirically) as [40]

$$\chi = \alpha + \beta/T \quad (9)$$

where α and β are constants. Therefore, by combing the values of d_{itp} with the SCFT from Eq. (1), the change of d_{itp} values with increasing temperature in all samples is qualitatively in good agreement with that of the theoretical predictions by Matsen et al. [8]. Surprisingly, we also found that the interphase thicknesses in these two block copolymers are obviously different. It is inconsistent with the theoretical predictions about the evolution of interphase in block copolymer melts by Matsen using self-consistent mean-field theory (SCFT) [8], where the (χ) parameters for the diblock and triblock systems were given identical values. This implies that the interphase thickness not only depends strongly on the binary thermodynamic interaction (χ) between the polystyrene (PS) and polybutadiene (PB) blocks, but also is influenced by their molecular architectures in the experimental temperature range where the two blocks are in the state of glass and melt, respectively.

It is noted that the interphase thickness of the SBS is bigger than that of the SB. To check the influence of the dimension parameter (p in Eq. (2)) in the calculation of d_{itp}, we compared the experimental

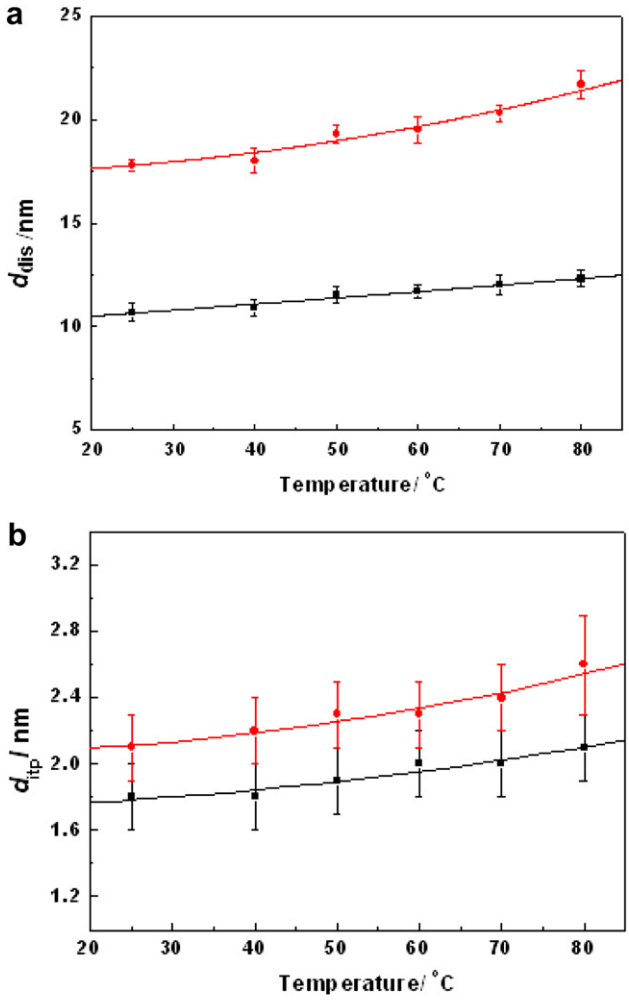

Fig. 8. Changes of the domain size (d_{dis}) dependence of the temperature (a) and dependence of interphase thickness (d_{itp}) on temperature (b) from 25 to 80 °C for SB (■) and SBS (●). The solid lines are least squares fits of experimental data.

results of d_{itp} using $p = 1$ (lamella) and 2 (cylinder) for SB and $p = 2$ (cylinder) and 3 (sphere) for SBS as shown in Figure S5 in Supplementary material. No obvious different of the d_{itp} can be found, which implies that the calculated d_{itp} is insensitive to the morphologies. While further theoretical work is needed for block copolymers where different blocks are in melt and glass state, respectively. So the χ parameters deduced by the SSNMR experiments combined with the theoretical calculation are looking forward to the developments of the SCFT for the non-melted block polymers.

The difference of the domain and interphase size in SB and SBS with the same S/B composition ratio should be correlated to the morphological difference as shown in Fig. 3, where SB exhibits lamellar but SBS does cylinder-type phase separation. In previous work on block copolymers using Monte Carlo simulations [41], it was found that ABA triblock chains can form loop and bridge configurations, therefore the arrangement of chain ends and segmental loops are different from those in diblocks, which would be origins for these morphological differences. On the other hand, TEM results shown in Fig. 3 also indicate that SBS is lack of long range order when compared with SB. This would be another reason for interphase size difference in the two copolymers.

4. Conclusions

In combination with other techniques, we have investigated the effect of temperature and molecular architecture on the interphase thickness and domain size of SB and SBS copolymers by ^{1}H SSNMR experiments in the temperature range from 25 to 80 °C. The domain size and the interphase thickness of the two block copolymers obviously increase with increasing temperature. It was found that the interphase thickness not only depended strongly on the binary thermodynamic interaction (χ) between the PS and PB blocks, but also is influenced by their molecular architectures in the experimental temperature range. This result was not agreement with that of the theoretical results by SCFT for polymer melts. We hope that our results may motivate further theoretical works on block copolymers where different blocks are in melt and glass state, respectively.

Our current NMR work on block copolymers and previous work on thermoset blends demonstrate that our improved ^{1}H spin-diffusion NMR technique for measuring the interphase thickness is a useful tool to elucidate the phase behavior and subtle microphase in multiphase polymers with obvious heterogeneous dynamics. By using this NMR method, the temperature dependence of the interphase thickness can also be captured to establish structure–property relationships of multiphase polymers.

Acknowledgments

This work was financially supported by National Natural Science Foundation of China (NSFC) through General Program (Nos. 20774054, 20374031), and National Science Fund for Distinguished Young Scholars (No. 20825416), and Program of New Century Excellent Talents in University (NCET-05-0221). The authors also thank engineer Yingjun Chen for her assistance with the SAXS measurements.

Appendix. Supplementary material

Supplementary material associated with this article can be found, in the online version, at doi: 10.1016/j.polymer.2010.03.009.

References

[1] Zumbulyadis N, Landry MR, Russell TP. Macromolecules 1996;29:2201–4.
[2] (a) Helfand E, Tagami YJ. Polym Sci Polym Lett 1971;9:741–6;
(b) Helfand E, Tagami Y. J Chem Phys 1972;56:3592–601;
(c) Helfand E, Sapse AM. J Chem Phys 1972;57:1812–3.
[3] Helfand E, Sapse AM. J Chem Phys 1975;62:1327–31.
[4] Broseta D, Fredrickson GH, Helfand E, Leibler L. Macromolecules 1990;23:132–9.
[5] Nedoma AJ, Robertson ML, Wanakule NS, Balsara NP. Macromolecules 2008;41:5773–9.
[6] Quan X, Bair HE, Johnson GE. Macromolecules 1989;22:4631–5.
[7] Willett JL, Wool RP. Macromolecules 1993;26:5336–49.
[8] (a) Matsen MW, Schick M. Phys Rev Lett 1994;72:2660–3;
(b) Matsen MW, Bates FS. Macromolecules 1996;29:1091–8.
[9] (a) Ruland W. Macromolecules 1987;20:87–93;
(b) Gemeinhardt GC, Moore RB. Macromolecules 2005;38:2813–9.
[10] Diamant J, Soong D, Williams MC. Polym Eng Sci 1982;22:673–83.
[11] Annighöfer F, Gronski W. Makromol Chem 1984;185:2213–31.
[12] Ni S, Zhang P, Wang Y, Winnik MA. Macromolecules 1994;27:5742–50.
[13] Shibayama M, Hashimoto T, Kawai H. Macromolecules 1983;16:1434–43.
[14] (a) Anastasiadis SH, Russell TP, Satija SK, Majkrzak CF. Phys Rev Lett 1989;62:1852–5;
(b) Anastasiadis SH, Russell TP, Satija SK, Majkrzak CF. J Chem Phys 1990;92:5677–91;
(c) Noro A, Okuda M, Odamaki F, Kawaguchi D, Torikai N, Takano A, et al. Macromolecules 2006;39:7654–61.
[15] Liu RYF, Bernal-Lara TE, Hiltner A, Baer E. Macromolecules 2004;37:6972–9.
[16] Higashida N, Kressler J, Yukioka S, Inoue T. Macromolecules 1992;25:5259–62.
[17] Merfeld GD, Paul DR. In: Paul DR, Bucknall CB, editors. Polymer blends: formulation and performance, 1. New York: Wiley; 2000. p. 55–60.
[18] Gobbi GC, Russell TP, Lyerla JR, Fleming WW, Nishi T. J Polym Sci Poly Lett 1987;25:61–76.
[19] (a) Farinha JPS, Vorobyova O, Winnik MA. Macromolecules 2000;33:5863–73;
(b) Liu RYF, Bernal-Lara TE, Hiltner A, Baer E. Macromolecules 2004;37:6972–9.
[20] Schmidt-Rohr K, Spiess HW. Multidimensional solid-state NMR and polymers. San Diego: Academic Press; 1994.
[21] (a) Kogler G, Mirau PA. Macromolecules 1992;25:598–604;
(b) Guo MM. Trends Polymer Sci 1996;4:238–44;
(c) VanderHart DL, Asano A, Gilman JW. Chem Mater 2001;13:3781–96;
(d) Mirau PA. A practical guide to understanding the NMR of polymers. Wiley-Interscience publisher; 2004;
(e) Kao HM, Chao SW, Chang PC. Macromolecules 2006;39:1029–40.
[22] (a) Sun PC, Dang QQ, Li BH, Chen TH, Wang YN, Lin H, et al. Macromolecules 2005;38:5654–67;
(b) Li XJ, Fu WG, Wang YN, Chen TH, Liu XH, Lin H, et al. Polymer 2008;49:2886–97.
[23] (a) Caravatti P, Neuenschwander P, Ernst RR. Macromolecules 1986;19:1889–95;
(b) Cho G, Natansohn A. Chem Mater 1997;9:148–54.
[24] Clauss J, Schmidt-Rohr K, Spiess HW. Acta Polym 1993;44:1–17.
[25] (a) Cho G, Natansohn A. Can J Chem 1994;72:2255–9;
(b) Cho G, Natansohn A, Ho T, Wynne KJ. Macromolecules 1996;29:2563–9.
[26] Landfester K, Boeffel C, Lambla M, Spiess HW. Macromolecules 1996;29:5972–80.
[27] Jack KS, Wang JH, Natansohn A, Register RA. Macromolecules 1998;31:3282–91.
[28] Cai WZ, Schmidt-Rohr K, Egger N, Gerharz B, Spiess HW. Polymer 1993;34:267–76.
[29] Saalwachter K, Thomann Y, Hasenhindl A, Schneider H. Macromolecules 2008;41:9187–91.
[30] Mirau PA, Yang S. Chem Mater 2002;14:249–55.
[31] Zhang QL, Tsui OKC, Du BY, Zhang FJ, Tang T, He TB. Macromolecules 2000;33:9561–7.
[32] Huang HY, Zhang FJ, Hu ZhJ, Du BY, He TB, Li KF, et al. Macromolecules 2003;36:4084–92.
[33] Nagapudi K, Leisen J, Beckham HW, Gibson HW. Macromolecules 1999;32:3025–33.
[34] Mellinger F, Wilhelm M, Spiess HW. Macromolecules 1999;32:4686–91.
[35] (a) Landfester K, Spiess HW. Acta Polym 1998;49:451–64;
(b) Egger N, Schmidt-Rohr K, Blumich B, Domke WD, Stapp B. J Appl Polym Sci 1992;44:289–95.
[36] Neagu C, Puskas JE, Singh MA, Natansohn A. Macromolecules 2000;33:5976–81.
[37] Demco DE, Johanson A, Tegenfeldt J. Solid State Nucl Magn Reson 1995;4:13–38.
[38] Hedesiu C, Demco DE, Kleppinger R, Buda AA, Blumich B, Remerie K, et al. Polymer 2007;48:763–77.
[39] (a) Horng TJ, Woo EM. Polymer 1998;39:4115–22;
(b) Hu LD, Lu H, Zheng SX. J Polym Sci B: Polym Phys 2004;42:2567–75.
[40] Rubinstein M, Colby RH. Polymer physics. New York: Oxford University Press; 2003.
[41] (a) Wang Z, Li BH, Jin QH, Ding DT, Shi AC. Macromol Theory Simul 2008;17:301–12;
(b) Wang Z, Li BH, Jin QH, Ding DT, Shi AC. Macromol Theory Simul 2008;17:86–102.